

Weierstraß-Institut
für Angewandte Analysis und Stochastik
Leibniz-Institut im Forschungsverbund Berlin e. V.

Preprint

ISSN 0946 – 8633

**Impact of interfacial slip on the stability of liquid two-layer
polymer films**

Sebastian Jachalski¹, Dirk Peschka¹, Andreas Münch², Barbara Wagner^{1,3}

submitted: November 21, 2012

¹ Weierstrass Institute
Mohrenstr. 39
10117 Berlin
Germany

E-Mail: sebastian.jachalski@wias-berlin.de
dirk.peschka@wias-berlin.de
barbara.wagner@wias-berlin.de

² Mathematical Institute
University of Oxford
24-29 St. Giles'
Oxford OX1 3LB, UK

E-Mail: muench@maths.ox.ac.uk

³ Institute of Mathematics
Technische Universität Berlin
Straße des 17. Juni 136
10623 Berlin
Germany

No. 1743
Berlin 2012



Key words and phrases. fluid dynamics, thin-film models, two-phase flow, interfacial slip.

The authors SJ, DP and BW are grateful for the support by the DFG of their project within the priority programme SPP 1506 "Transport at Fluidic Interfaces".

Edited by
Weierstraß-Institut für Angewandte Analysis und Stochastik (WIAS)
Leibniz-Institut im Forschungsverbund Berlin e. V.
Mohrenstraße 39
10117 Berlin
Germany

Fax: +49 30 20372-303
E-Mail: preprint@wias-berlin.de
World Wide Web: <http://www.wias-berlin.de/>

Abstract

In this study systems of coupled thin-film models for two immiscible liquid polymer layers on a solid substrate that account for interfacial slip and intermolecular forces are derived. On the scale of tens to hundred nanometers such two-layer systems are susceptible to instability and may rupture and dewet. The stability of the two-layer system and its significant dependence on the order of magnitude of slip is investigated via these thin-film models. With no-slip at both, the liquid-liquid and liquid-solid interface and polymer layers of comparable thickness, the dispersion relation typically shows two local maxima, one in the long-wave regime and the other at moderate wavenumbers. The former is associated with perturbations that mainly affect the gas-liquid interface and the latter with higher relative perturbation amplitudes at the liquid-liquid interface. Slip at the liquid-liquid interface generally favors the former perturbations. However, when the liquid-liquid and the liquid-solid interface exhibit large slip, the maxima shift to small wavenumbers for increasing slip and hence may significantly change the spinodal patterns.

1 Introduction

The stability of thin liquid films is of great interest in many technological applications involving lubricants and coatings. In particular, when the thickness of the films is on the micro- to nanoscale, bulk and surface stresses compete with intermolecular forces and may lead to complex wetting or dewetting dynamics. Understanding and controlling this dynamics is fundamental in nanoscale design and functionalisation of surfaces for numerous applications ranging from optoelectronics to biotechnology. However, while stability, rupture and dewetting processes of liquid films from solid substrates have been investigated intensively experimentally and theoretically during the past decades, there are comparatively fewer studies for two-layer immiscible liquid films. Moreover, two-layer liquid films have a far richer dynamics and potentially more complex morphological structures even when both liquid layers are Newtonian. Here, apart from differences in thickness and density of the two layers, additional parameters such as the ratio of the viscosities of both liquids, and the ratio of interfacial tensions can play the dominant role on the morphological structure.

Some of these effects are explored in an early experimental and theoretical study on liquid-liquid dewetting in Brochard-Wyart et al. [1]. Two-layer systems were investigated by linear stability analysis as well as numerical simulations including rupture. In a series of publications by Pototsky et al. [2, 3], Fisher & Golovin [4, 5], Bandyopadhyay et al. [6, 7] and Craster & Matar [8] in the framework of lubrication theory. Also, stationary droplet solutions for liquid-liquid systems and their stability have been studied numerically for the coupled system of thin film equations by Pototsky et al. [3]. Many more studies are found in a recent comprehensive review on both single and two-layer systems by Craster & Matar [9], illustrating the extent of work in this field.

Interestingly, interfacial slip between immiscible, liquid polymer layers has not been taken into account in the framework of two-layer thin-film models, even though already the work by Lin [10] suggested the possibility of interfacial slip, and a number of experimental studies have demonstrated clear evidence of slip at polymer-polymer interfaces. Most importantly, we mention here the coextrusion experiments by Zhao & Macosko [11] that exhibit slip, in particular between polystyrene (PS) and polymethylmethacrylate (PMMA) interfaces, also more recent measurements by Zeng et al. [12], and in liquid two-layer systems of PS dewetting from PMMA by Lin et al. [13]. On the other hand, the intensely investigated slip phenomena for thin polymer films on solid substrates, for example as it occurs when a polymer film dewets a hydrophobically coated substrate, has often been described by a Navier-Slip condition, relating the lateral velocity along the substrate to the shear rate $u = b u_z$ with the extrapolation length b being a measure of the slip length. In fact, b is an apparent slip length being a measure of an underlying microscopic mechanism. A well-known example is the case of polymer melts dewetting from a monolayer of polymer chains grafted on a substrate, for which Brochard & De Gennes [14] showed that b can be derived from microscopic consideration as a coil-stretch transition into a disentangled state with much lower Rouse friction, and hence viscosity, within a very thin layer near the substrate. Other mechanisms corresponding to other liquid-solid systems exhibiting apparent slip are described in Léger [15] and the review by Lauga et al. [16].

While these results are of fundamental importance, they have also led to the derivation of new thin-film models, in particular for dewetting polymer melts, that take into account apparent slip of various orders of magnitude. The investigations by Kargupta et al. [17] showed a strong dependence of the time scale of rupture and density of holes of the typically unstable polymer film. In Münch et al. [18] and Fetzer et al. [19] it was shown that the dynamics and morphology of dewetting rims may even be controlled by slippage. Their models systematically explained experimental results on the shape of the rim that were previously attributed to viscoelastic effects [20, 21] and moreover established a new experimental method for assessing slip in thin polymer films [22, 23].

Thin-film models for immiscible polymer layers taking into account orders of magnitude of interfacial slip are the main topic of this study and make use of the theories and analysis of the microscopic mechanisms at the polymer-polymer interface under shearing motion. The derivation of apparent slip at polymer-polymer interfaces has been developed in work by Goveas & Fredrickson [24], Adhikari & Goveas [25] extending earlier work by De Gennes, Brochard-Wyart and Ajdari [26, 27, 28] for unentangled polymer, entangled polymer, dilute polymer emulsions, as well as for cases when both liquid layers are Newtonian. In essence, the repulsive forces within a thin interfacial region of two immiscible polymer films introduce higher shear rates and hence an apparent velocity discontinuity leading to the concept of apparent slip.

As for single polymer layers on a solid substrate, the dimension-reduced thin film models allow for the systematic analysis of early to long-time dynamics and the numerical simulation of the morphological evolution and stability analysis of the interfaces. After the derivation of the thin film models that take account of orders of magnitude of slip, we will focus on the stability analysis about flat constant interfaces. The main tasks here are to determine the dispersion relations and the dominant spinodal wavelength and to determine the mode of the perturbation of the two interfaces, such as zig-zag or varicose. Because the base states are constant it is straight

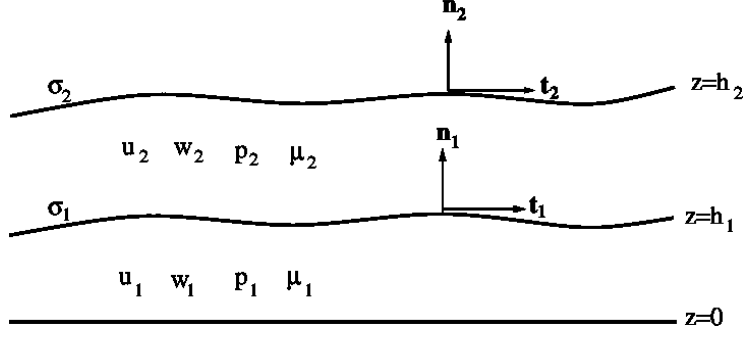


Figure 1: Sketch of a two-layer system

forward, though lengthy, to carry out a linear stability analysis for the underlying Stokes problem, which is included in an appendix. This was done with the aim to assure that the stability results for the new thin-film models are obtained as limiting cases of the underlying stability problem for the Stokes equations.

Although there are number of potential combinations of slip conditions for different orders of magnitude at the solid substrate and the liquid-liquid interface, we analyse here two models, which show most clearly the significant impact of interfacial slip on the stability behavior of the liquid-liquid system. In particular, we discuss the case when strong-slip conditions are imposed at both interfaces, with a strong coupling of the dynamics of the interfaces. We note, that for other combinations, such as weak- or no-slip at the solid substrate and strong-slip at the liquid-liquid interface, the systems of thin-film equations decouple.

2 Formulation

The basic situation where two liquid layers are deposited on a solid substrate is depicted in fig. 1. Coordinates are introduced with the x -axis pointing in the lateral direction, along the flat solid substrate, and the z axis pointing normal to it. The solid-liquid interface is located at $z = 0$ and the liquid-liquid and liquid-gas interface at $z = h_1(x, t)$ and $z = h_2(x, t)$, respectively, where t denotes time. The variables u_i, w_i and p_i denote the lateral and vertical velocity components, and the pressure, respectively in the i -th layer, with $i = 1, 2$. The viscosity is denoted by μ_i , $i = 1, 2$ for the two layers. Surface tension for the liquid-liquid and liquid-gas interface are given by σ_1 and σ_2 , respectively.

In both layers, we have the Navier-Stokes and mass conservation equations for incompressible Newtonian liquids,

$$\rho \frac{du_i}{dt} = -\partial_x p_i + \mu_i (\partial_{xx} u_i + \partial_{zz} u_i), \quad (2.1a)$$

$$\rho \frac{dw_i}{dt} = -\partial_z p_i + \mu_i (\partial_{xx} w_i + \partial_{zz} w_i), \quad (2.1b)$$

$$\partial_x u_i + \partial_z w_i = 0, \quad (2.1c)$$

where d/dt is the material derivative in each layer, $d/dt = \partial_t + u_i \partial_x + w_i \partial_z$, and $i = 1, 2$. For simplicity, we assume that both layers have the same density ρ . At the substrate $z = 0$, we

impose the Navier-slip condition with slip-length b_1 and the impermeability condition,

$$u_1 = b_1 \partial_z u_1, \quad w_1 = 0. \quad (2.2a)$$

The free surface $z = h_2(x, t)$ evolves with the flow according to the kinematic condition,

$$(0, \partial_t h_2) \cdot \mathbf{n}_2 = (u_2, w_2) \cdot \mathbf{n}_2, \quad (2.2b)$$

and the tangential and normal stress condition, which are, respectively,

$$\mathbf{n}_2 \cdot (\Pi_2 + \phi'(h)I) \cdot \mathbf{t}_2 = 0, \quad (2.2c)$$

$$\mathbf{n}_2 \cdot (\Pi_2 + \phi'(h)I) \cdot \mathbf{n}_2 = \sigma_2 \kappa_2 \cdot \mathbf{n}_2. \quad (2.2d)$$

Similarly, at the liquid-liquid interface $z = h_1(x, t)$, we have the kinematic condition, tangential and normal stress condition, and the impermeability and slip condition with slip length b , which are, respectively,

$$(0, \partial_t h_1) \cdot \mathbf{n}_1 = (u_1, w_1) \cdot \mathbf{n}_1, \quad (2.3a)$$

$$\mathbf{n}_1 \cdot (\Pi_1 - \Pi_2 - \phi'(h)) \cdot \mathbf{t}_1 = 0, \quad (2.3b)$$

$$\mathbf{n}_1 \cdot (\Pi_1 - \Pi_2 - \phi'(h)) \cdot \mathbf{n}_1 = \sigma_1 \kappa_1 \cdot \mathbf{n}_1, \quad (2.3c)$$

$$(u_2 - u_1, w_2 - w_1) \cdot \mathbf{n}_1 = 0, \quad (2.3d)$$

$$(u_2 - u_1, w_2 - w_1) \cdot \mathbf{t}_1 = b \left(\frac{1}{\mu_1} + \frac{1}{\mu_2} \right) \mathbf{n}_1 \cdot \Pi_2 \cdot \mathbf{t}_1. \quad (2.3e)$$

Here we denote the thickness of the top layer by

$$h(x, t) = h_2(x, t) - h_1(x, t), \quad (2.4)$$

the stress and strain tensors in the i -th layer $i = 1, 2$, by

$$\Pi_i = -p_i I + \mu_i \hat{\gamma}_i, \quad \text{where} \quad \gamma_i = \partial_j u_{ik} + \partial_k u_{ij}, \quad (2.5)$$

and the unit tangential and normal vectors and curvature of the two interfaces $i = 1, 2$ by

$$\mathbf{n}_i = \frac{(-\partial_x h_i, 1)}{\sqrt{1 + (\partial_x h_i)^2}}, \quad \mathbf{t}_i = \frac{(1, \partial_x h_i)}{\sqrt{1 + (\partial_x h_i)^2}}, \quad \kappa_i = \nabla \cdot \mathbf{n}_i. \quad (2.6)$$

We focus on a situation where the contributions to the surface forces from the interaction with the solid substrate can be neglected, but the interaction with the bottom layer is relevant and can drive spinodal dewetting. Since these interactions decrease with the thickness of the bottom and the top layer, respectively, this can be achieved, for example, by considering thin enough top layers and only moderately thin bottom layers. The intermolecular potential for the interactions is thus given by

$$\phi(h) = \frac{8}{3} \phi_* \left[\frac{1}{8} \left(\frac{h_*}{h} \right)^8 - \frac{1}{2} \left(\frac{h_*}{h} \right)^2 \right]. \quad (2.7)$$

The h^{-2} term represents the disjoining pressure contribution from the van-der-Waals forces that promotes dewetting, while the h^{-8} term is relevant only at very small thicknesses and is stabilising. In fact, the potential has a minimum $\phi_* < 0$ at $h = h_*$.

2.1 Nondimensional Problem

Let H denote the typical thickness of the upper layer, i.e. of $h_2 - h_1$, and let L , U and P be a characteristic lateral length, velocity and pressure scale. We introduce these scalings via

$$\left. \begin{aligned} x &= L\tilde{x}, & z &= H\tilde{z}, & h_i &= H\tilde{h}_i, & b &= H\tilde{b}, & b_1 &= H\tilde{b}_1, \\ u_i &= U\tilde{u}_i, & w_i &= W\tilde{w}_i, & t &= \frac{L}{U}\tilde{t}, \\ p_i &= P\tilde{p}_i, & \phi' &= P\tilde{\phi}'. \end{aligned} \right\} \quad (2.8)$$

and then drop ' \sim '. A pressure scale is set by the derivative of the intermolecular potential. The choice

$$P = \frac{8\phi_*}{3H}, \quad (2.9)$$

results in a particularly simple form for ϕ' ,

$$\phi'(h) = \frac{1}{\varepsilon} \left[-\left(\frac{\varepsilon}{h}\right)^9 + \left(\frac{\varepsilon}{h}\right)^3 \right], \quad \text{where } \varepsilon = \frac{h_*}{H}. \quad (2.10)$$

For the equations in the bulk of the liquid layers, we obtain

$$\varepsilon_\ell \text{Re} \frac{du_2}{dt} = -\alpha \varepsilon_\ell \partial_x p_2 + \varepsilon_\ell^2 \partial_{xx} u_2 + \partial_{zz} u_2, \quad (2.11a)$$

$$\varepsilon_\ell^2 \text{Re} \frac{dw_2}{dt} = -\alpha \partial_z p_2 + \varepsilon_\ell^3 \partial_{xx} w_2 + \varepsilon_\ell \partial_{zz} w_2, \quad (2.11b)$$

$$0 = \partial_x u_2 + \partial_z w_2, \quad (2.11c)$$

$$\varepsilon_\ell \text{Re} \frac{du_1}{dt} = -\alpha \varepsilon_\ell \partial_x p_1 + \mu \left(\varepsilon_\ell^2 \partial_{xx} u_1 + \partial_{zz} u_1 \right), \quad (2.11d)$$

$$\varepsilon_\ell^2 \text{Re} \frac{dw_1}{dt} = -\alpha \partial_z p_1 + \mu \left(\varepsilon_\ell^3 \partial_{xx} w_1 + \varepsilon_\ell \partial_{zz} w_1 \right), \quad (2.11e)$$

$$0 = \partial_x u_1 + \partial_z w_1. \quad (2.11f)$$

At the free surface $z = h_2$ we get for the normal, tangential and kinematic condition, respectively

$$\begin{aligned} p_2 - \phi'(h) + \frac{\partial_{xx} h_2}{\left[1 + \varepsilon_\ell^2 (\partial_x h_2)^2\right]^{3/2}} \\ = 2 \frac{\varepsilon_\ell}{\alpha} \frac{\left[1 - \varepsilon_\ell^2 (\partial_x h_2)^2\right] \partial_z w_2 - \left[\partial_z u_2 + \varepsilon_\ell^2 \partial_x w_2\right] \partial_x h_2}{1 + \varepsilon_\ell^2 (\partial_x h_2)^2}, \end{aligned} \quad (2.11g)$$

$$\left[\partial_z u_2 + \varepsilon_\ell^2 \partial_x w_2\right] \left[1 - \varepsilon_\ell^2 (\partial_x h_2)^2\right] - 4\varepsilon_\ell^2 \partial_x u_2 \partial_x h_2 = 0, \quad (2.11h)$$

$$\partial_t h_2 = w_2 - u_2 \partial_x h_2. \quad (2.11i)$$

For the boundary condition at the free liquid-liquid interface $z = h_1$ we get for the normal, tangential and kinematic condition, respectively

$$\begin{aligned} p_1 - p_2 + \phi'(h) + \sigma \frac{\partial_{xx} h_1}{\left[1 + \varepsilon_\ell^2 (\partial_x h_1)^2\right]^{3/2}} \\ = 2 \frac{\varepsilon_\ell}{\alpha} \frac{\left[1 - \varepsilon_\ell^2 (\partial_x h_1)^2\right] \partial_z (\mu w_1 - w_2) - \left[\partial_z (\mu u_1 - u_2) + \varepsilon_\ell^2 \partial_z (\mu w_1 - w_2)\right] \partial_x h_1}{1 + \varepsilon_\ell^2 (\partial_x h_1)^2}, \end{aligned} \quad (2.11j)$$

$$\left[\partial_z (\mu u_1 - u_2) + \varepsilon_\ell^2 \partial_x (\mu w_1 - w_2) \right] \left[1 - \varepsilon_\ell^2 (\partial_x h_1)^2 \right] - 4\varepsilon_\ell^2 \partial_x (\mu u_1 - u_2) \partial_x h_1 = 0, \quad (2.11k)$$

$$\partial_t h_1 = w_1 - u_1 \partial_x h_2. \quad (2.11l)$$

The impermeability condition between the upper and lower liquid layer is given by

$$(w_2 - w_1) - (u_2 - u_1) \partial_x h_1 = 0. \quad (2.11m)$$

The slip condition at the liquid-liquid interface becomes

$$(u_2 - u_1) + \varepsilon_\ell^2 (w_2 - w_1) \partial_x h_1 = b \frac{\mu + 1}{\mu} \frac{[\partial_z u_2 + \varepsilon_\ell^2 \partial_x w_2] \left[1 - \varepsilon_\ell^2 (\partial_x h_1)^2 \right] - 4\varepsilon_\ell^2 \partial_x u_2 \partial_x h_1}{\sqrt{1 + \varepsilon_\ell^2 (\partial_x h_1)^2}}, \quad (2.11n)$$

and the boundary conditions (impermeability and Navier-slip) at the substrate are

$$w_1 = 0, \quad u_1 = b_1 \partial_z u_1. \quad (2.11o)$$

Here we denote

$$\varepsilon_\ell = \frac{H}{L}, \quad \text{Re} = \frac{\rho U H}{\mu_2}, \quad \mu = \frac{\mu_1}{\mu_2}, \quad \sigma = \frac{\sigma_1}{\sigma_2}, \quad \alpha = \frac{P H}{\mu_2 U}. \quad (2.12)$$

When balancing equation (2.11g), we have set, without loss of generality,

$$\frac{\sigma_2 H}{P L^2} = 1 \quad (2.13)$$

Together with (2.9), we then find

$$\varepsilon_\ell = \frac{H}{L} = \sqrt{\frac{8 \phi_*}{3 \sigma_2}}. \quad (2.14)$$

Throughout this paper, we assume that $\varepsilon_\ell \ll 1$, and derive thin film equations for the profiles h_2 and h_1 for various degrees of slip at the solid-liquid and the liquid-liquid interfaces. Different magnitudes of the slip lengths will require different choices for α in terms of the small parameter ε_ℓ . We will treat μ and σ as order one parameters. For many systems, such as dewetting micro- and nanoscopic polymer films, inertia is negligibly small. Therefore, we will only cover the case $\text{Re} = 0$, but remark that keeping inertia can be done easily for the strong-slip models in appropriate regimes of Re , analogous to one layer models [18].

3 Thin-film models

3.1 Weak-slip case

In this section we assume that during the dewetting motion of the upper layer from the lower layer will exhibit no-slip at the interface $z = h_1$, i.e. we set $b_1 = 0$ in (2.11o), and we wish to

vary slip at the liquid-liquid interface. We will refer to the resulting thin film model as the no-slip weak-slip model (NS-WS model). In this case the flow is driven by the lateral pressure gradient $\partial_x p$ acting on the dominant viscous term $\partial_{zz} u_2$ in (2.11a). Thus we balance the two by letting

$$\alpha = \frac{1}{\varepsilon_\ell}, \quad (3.1)$$

which fixes the velocity scale and thus the capillary number in terms of ε_ℓ ,

$$\text{Ca} = \frac{\mu_2 U}{\sigma_2} = \varepsilon_\ell^3. \quad (3.2)$$

The corresponding leading order problem in (2.11) can then be integrated and reduced to the system of partial differential equations for $h_2(x, t)$ and $h_1(x, t)$ using the kinematic conditions (2.11i) and (2.11l). The derivation is a straight forward variation of the case where there is no-slip at both interfaces, see e.g. [2, 8]. Here we find it more convenient to write the thin-film model as a system for $h_1(x, t)$ and $h(x, t) = h_2(x, t) - h_1(x, t)$. To do this note that

$$\partial_t h = -\partial_x \int_{h_1}^{h_2} u_2 dz, \quad (3.3)$$

and obtain

$$\partial_t h_1 = \frac{1}{\mu} \partial_x \left[\frac{h_1^3}{3} \partial_x p_1 + \frac{h_1^2}{2} h \partial_x p_2 \right], \quad (3.4a)$$

$$\partial_t h = \partial_x \left[\left(\frac{1}{3} h^3 + \frac{\mu+1}{\mu} b h^2 \right) \partial_x p_2 + \frac{1}{\mu} \frac{h_1^2}{2} h \partial_x p_1 + \frac{1}{\mu} h_1 h^2 \partial_x p_2 \right], \quad (3.4b)$$

where

$$\partial_x p_1 = -(\sigma+1) \partial_x \left(\partial_{xx} h_1 + \frac{1}{\sigma+1} \partial_{xx} h \right), \quad (3.4c)$$

$$\partial_x p_2 = -\partial_x \left(\frac{\sigma}{\sigma+1} \partial_{xx} h - \phi'(h) \right) + \frac{1}{\sigma+1} \partial_x p_1. \quad (3.4d)$$

This can be written as

$$\partial_t \mathbf{h} = \partial_x (Q \cdot \partial_x \mathbf{p}), \quad (3.5a)$$

where \mathbf{h} denotes the vector $(h_1(x, t), h(x, t))$, $\mathbf{p} = (p_1(x, t), p_2(x, t))$, and Q the mobility matrix given by

$$Q = \frac{1}{\mu} \begin{bmatrix} \frac{h_1^3}{3} & \frac{h_1^2 h}{2} \\ \frac{h_1^2 h}{2} & \frac{\mu}{3} h^3 + (\mu+1) b h^2 + h_1 h^2 \end{bmatrix}. \quad (3.5b)$$

Note also, that (3.4c) and (3.4d) are equivalent to

$$\partial_x p_2 = -\partial_x (\partial_{xx} h_2 - \phi'(h)) \quad (3.6a)$$

$$\partial_x p_1 = -\partial_x (\sigma \partial_{xx} h_1 + \phi'(h)) + \partial_x p_2 = -\partial_x (\sigma \partial_{xx} h_1 + \partial_{xx} h_2) \quad (3.6b)$$

3.2 Strong-slip case

We now assume that during the dewetting motion of the upper from the lower layer there is significant slip at both the solid substrate and the liquid-liquid interface. The systematic derivation of one-layer thin film models for different regimes of slip at the substrate [18] has shown that the case of strong slip, where the dimensionless slip length is $O(\varepsilon_\ell^{-2})$, represents a distinguished limit. It leads to a particularly rich model that incorporates the effect of elongational stresses. We therefore consider strong slip at both $z = 0$ and $z = h_1$ and introduce slip parameters of $O(\varepsilon_\ell^{-2})$ at the bottom and liquid-liquid interface, respectively

$$b_1 = \frac{\beta_1}{\varepsilon_\ell^2}, \quad b = \frac{\beta}{\varepsilon_\ell^2}. \quad (3.7)$$

Also, guided by the derivation [18], the plug-flow scaling in both layers leads to $Ca = \varepsilon_\ell$ and thus here $\alpha = \varepsilon_\ell$. Expanding all dependent variables in terms of ε_ℓ^2 , we find that to leading order, the lateral velocity fields u_i turn out to be constant in z , i.e. we have plug flow in both layers. To obtain closed form thin-film models for h , h_1 and the lateral velocities u_1 and u_2 the derivation needs to consider also the problem to $O(\varepsilon_\ell^2)$ in order to obtain solvability conditions. The resulting velocity fields and the leading order film profiles $h_1(x, t)$ and $h(x, t)$ satisfy the following system of equations,

$$0 = -\partial_x (-(\sigma + 1) \partial_{xx} h_1 - \partial_{xx} h) + \frac{4\mu}{h_1} \partial_x (\partial_x u_1 h_1) + \frac{\mu(u_2 - u_1)}{(\mu + 1)\beta h_1} - \frac{\mu u_1}{\beta_1 h_1}, \quad (3.8a)$$

$$\partial_t h_1 = -\partial_x (h_1 u_1), \quad (3.8b)$$

$$0 = -\partial_x (\phi'(h) - \partial_{xx} h_1 - \partial_{xx} h) + \frac{4}{h} \partial_x [\partial_x u_2 h] - \frac{\mu(u_2 - u_1)}{(\mu + 1)\beta h}, \quad (3.8c)$$

$$\partial_t h = -\partial_x (h u_2). \quad (3.8d)$$

We avoid interruption of the flow of argument and include the details of the derivation of this new model in appendix B.

4 Linear stability

4.1 Dispersion relation for the no-slip weak-slip model

We investigate the stability of the stationary solution with two flat interfaces. Since we have assumed in the non-dimensionalisation (2.8) that the length scale H is the typical thickness of

the top liquid layer, the base state is given by

$$h_1(x, t) = h_1^0, \quad h(x, t) = 1.$$

We introduce normal mode perturbations according to

$$h_1(x, t) = h_1^0 + \delta\chi_1 \exp(jkx + \omega t), \quad h(x, t) = 1 + \delta(\chi_2 - \chi_1) \exp(jkx + \omega t),$$

where $j = \sqrt{-1}$ is the imaginary unit, k the wavenumber and ω the growth rate of the normal mode perturbation, respectively, and $0 < \delta \ll 1$. The notation is chosen to be consistent with expansions where perturbations $\delta\chi_1 \exp(jkx + \omega t)$ and $\delta\chi_2 \exp(jkx + \omega t)$ are applied to h_1 and h_2 , respectively. Substituting this into (3.4) after eliminating p_1 and p_2 , expanding to first order in terms of δ , and dropping the superscript '0', we obtain the following eigenproblem for the eigenvalue ω and the eigenvector $\bar{\chi} = (\chi_1, \chi_2 - \chi_1)$,

$$\omega \bar{\chi} = -k^2 Q E \bar{\chi} \quad (4.1)$$

where Q is the mobility matrix (3.5b) with $h = 1$, and

$$E = \begin{bmatrix} (\sigma + 1)k^2 & k^2 \\ k^2 & k^2 + \phi''(1) \end{bmatrix}. \quad (4.2)$$

Therefore, the dispersion relation is given by

$$\omega_{1,2} = -\frac{k^2}{2} \text{Tr}(\bar{Q}E) \pm k^2 \sqrt{\frac{\text{Tr}(\bar{Q}E)^2}{4} - \text{Det}(\bar{Q}E)}. \quad (4.3)$$

For each value of k , there two eigenvalues. These always turned out to be real, and then have different sign if $\det E < 0$. In fact, one eigenvalue is positive (and the other negative) if $k < k_c$, and both are stable for $k > k_c$, where the ‘‘cut-off’’ wavenumber k_c is obtained from the condition $\det E = 0$ with the result

$$k_c = \left[\frac{\sigma + 1}{\sigma} \right]^{1/2}. \quad (4.4)$$

4.1.1 No slip: $b = 0$.

To provide a baseline, we first investigate how the dispersion relations and the corresponding perturbations of the two interfaces are affected by different thicknesses h_1 of the lower layer in the case when there is no slip at all, $b = 0$. In many practical situations, the surface tension of the liquid-liquid interface is lower by an order of magnitude than of the gas-liquid interface. We therefore choose a small value for $\sigma = 0.1$. For simplicity, we assume that the two liquids have the same viscosity, i.e. $\mu = 1$. Moreover, the value of $|\phi''(1)|$ can be scaled out of the problem by rescaling $k = |\phi''(1)|^{1/2} \tilde{k}$ and $\omega = |\phi''(1)|^2 \tilde{\omega}$, thus, we can set $\phi'' = -1$ without losing generality. With these parameters, $k_c = 3.32$.

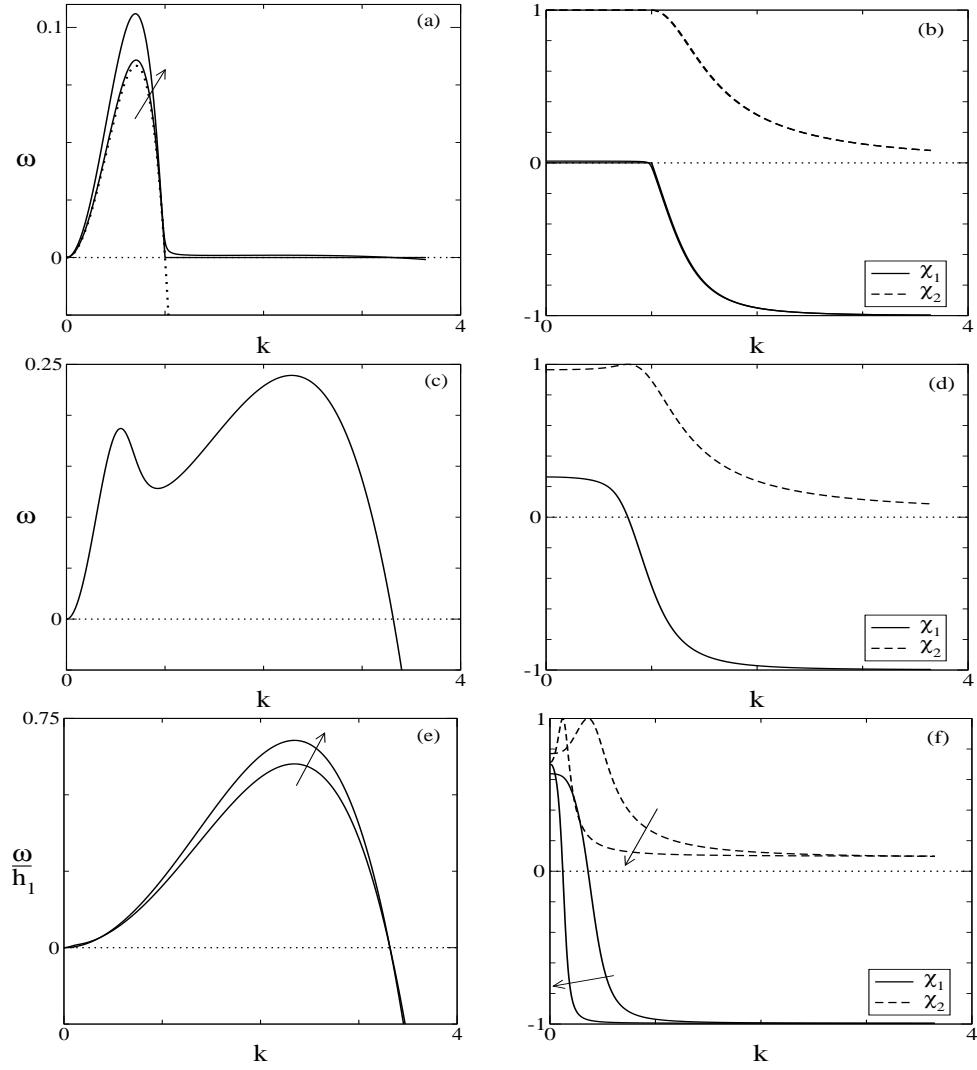


Figure 2: Dispersion relations (left column ((a), (c), (e))) and components of the perturbation vector (right column ((b), (d), (f))) for no-slip at both interfaces. The film thickness of the bottom layer is varied from top to bottom, with $h_1 = 0.1, 0.01$ in the top row, $h_1 = 1$ in the middle and $h_1 = 10, 100$ in the bottom row. Arrows point in the direction of larger h_1 . Values for other parameters are stated in the main text. The two components χ_1 and χ_2 of the perturbation vector correspond to perturbations of the liquid-liquid and gas-liquid interface, and have been normalised so that $\chi_1^2 + \chi_2^2 = 1$.

For moderate thickness of the lower layer ($h_1 = 1$), the most prominent feature to observe are the two maxima in the dispersion relation in fig. 2(c), suggesting a bimodal instability with two different wavelengths. Such a dispersion relation with two maxima was also observed by Pototsky et al. [2] for a situation with three interaction potentials and no-slip at both interfaces. Inspection of the components of the perturbation vector $\bar{\chi}$ reveals a transition in the shape of the perturbed layers as k increases from the range where ω has its first maximum to where it has the second maximum. For k less than about one, the shape of the perturbation is zig-zag like (both interfaces are perturbed in the same direction), and for k larger than about one, it is varicose. However, the modes are quite asymmetric. For the $k \geq 2$, the gas-liquid is only weakly perturbed and in fact the relative amplitude compared to the perturbation of the liquid-liquid interface tends to zero if σ is made smaller. This is plausible, since $\sigma \rightarrow 0$ implies a very stiff gas-liquid interface, $\sigma_2 \gg \sigma_1$. For longer wavelengths, surface tension should be less important at both interfaces, so that the stability is governed by the intermolecular forces and geometrical constraints i.e. the presence of a solid substrate below the bottom layer. The latter is expected to have a stronger suppressing effect on the liquid-liquid interface deformation, thus for $k < 1$, the gas-liquid interface is perturbed more strongly than the liquid-liquid interface.

For small values of the thickness of the lower layer, $h_1 = 0.1$ and $h_1 = 0.01$, we expect the impact of geometric constraints to be more relevant closer to the substrate. Indeed, for k less than about one, the zig-zag mode in fig. 2(b) is more asymmetric than previously in fig. 2(d), with $\chi_2 = O(h_1^2)$, so that in the limit $h_1 \rightarrow 0$, only the gas-liquid interface is perturbed. We then have a transition in the relative amplitudes for k between one and two as before. In fact, the relative amplitudes for larger k are very similar to those in fig. 2(d). However, if we look at the dispersion relation fig. 2(a), the growth rates for $k > 1$ are small, so that the range of wave-numbers where the perturbations predominantly affect the bottom (liquid-liquid) interface are nearly stable. Thus, the geometric constraints suppress the instability in this range of k and eliminate one of the maxima present for moderate h_1 . For $k < 1$, the shape of the perturbation suggest a behaviour as in a one-layer system and indeed, an asymptotic analysis shows that for $h_1 \ll 1$, one eigenvalue is

$$\omega_{\text{asy}} = -\frac{1}{3}k^2(k^2 - 1) \quad (4.5)$$

to leading order, the other is zero (i.e. not order one in h_1). The relation (4.5) has its maximum at the wavenumber $k = \sqrt{1/2}$ and its cut-off wavenumber at 1. The top eigenvalue ω_1 approaches ω_{asy} from above for $k < 1$ and the zero eigenvalue, for $k > 1$. It therefore has its maximum near $k = \sqrt{1/2}$ and is nearly zero, but still positive, for $k > 1$ up to k_c , after which it is stable (i.e. negative).

For large $h_1 = 10$ and $h_1 = 100$, the other maximum in the dispersion relation wins, see fig. 2(e). For the wave-numbers where it is located, the shape of the perturbation is that of a varicose mode where the perturbation affects both interfaces in opposite directions. However, due to the smallness of σ , the gas-liquid interface is much stiffer than the liquid-liquid interface thus the effect of the perturbation on the former is small. In the long wave regime, the shape of the perturbations is zig-zag like and is increasingly symmetric i.e. it affects both interfaces equally well as $h_1 \rightarrow \infty$. The region of k with the zig-zag shape in fig. 2(f) is thinner than for previously discussed h_1 , of order $O(h_1^{-1/2})$. Notice that growth rates in this regime for k are small compared to the maximum rates achieved for $k > 1$.

Summarising, we have for moderate thickness h_1 and small σ , i.e. relatively soft liquid-liquid interface, a bimodal instability. The longer-wave maximum corresponds to a one-layer model where the perturbations occur mainly at the liquid-gas interface while they are inhibited at the liquid-liquid interface due to the constraints from the presence of the substrate. The shorter-wave maximum corresponds to the dominant mode of a one-layer system of thickness $h = 1$ with two interfaces at a distance from any solid substrate. The instability is dominant at the softer i.e. the liquid-liquid interface. The lower surface tension of this interface determines the preferred wavelength.

4.1.2 General b .

We now investigate how the dispersion relation and perturbation shapes change, for moderate, small and large h_1 , if b is increased. All other parameter values are retained from the previous numerical experiments. Starting with $h_1 = 1$, in fig. 3(d), we notice that the components of the perturbation vector shown in (b) change comparatively little. The transition from an asymmetric zig-zag to an asymmetric varicose shape at $k = 1 \dots 2$ that was already observed for $b = 0$ persists for larger slip. At the upper end of the k shown, the graphs for χ_1 and χ_2 are very similar. The strongest dependence on b is seen for $k < 1$, where $\chi_1 \rightarrow 0$ as $b \rightarrow \infty$, i.e. the already weak coupling between the interfaces is further diminished.

In the dispersion relation fig. 3(c), increasing b increases ω (notice the scaling of ω with $(1 + b)$). This is to be expected, since this decreases friction, which accelerates the evolution of the instability. However, the values for ω with k less than about one increase like $\propto b$ for $b \rightarrow \infty$, while the increase of ω for wavenumbers larger than one is smaller. This is not surprising, since the lower- k instability mainly involves the gas-liquid interface (as seen in (b)), for which the friction reduction is stronger than for the liquid-liquid interface which is more directly affected by the no-slip condition at the solid substrate. The preferential increase of the growth rates allows the lower- k instability to eventually overtake the larger- k instability.

For small $h_1 = 0.1$, we therefore expect that the lower- k instability is further reinforced. Indeed, the dispersion relation in fig. 3(a) does not change qualitatively with increasing b , except that the maximum growth rates increase approximately linearly in b for larger slip lengths. The shape of the perturbations are hardly affected by changes in b over two orders of magnitude, as shown in fig. 3(b), where the lines for χ_1 and for χ_2 for the different b nearly coincide.

The effect of increasing b is more dramatic for larger h_1 . For $h_1 = 10$ and $b = 0$, the dispersion relation fig. 3(e) has only one maximum at k larger than one, with a preferential perturbation of the liquid-liquid interface (see fig. 3(f)). As b is increased, the lower- k maximum appears again, for the instability that mainly affects the gas-liquid interface. Thus, we recover a bimodal situation. As b is increased even further, the lower- k maximum eventually dominates. Thus we transition from a shorter wavelength perturbation that affects mainly the liquid-liquid interface to a longer wavelength perturbation of predominantly the gas-liquid interface simply by increasing the slip length.

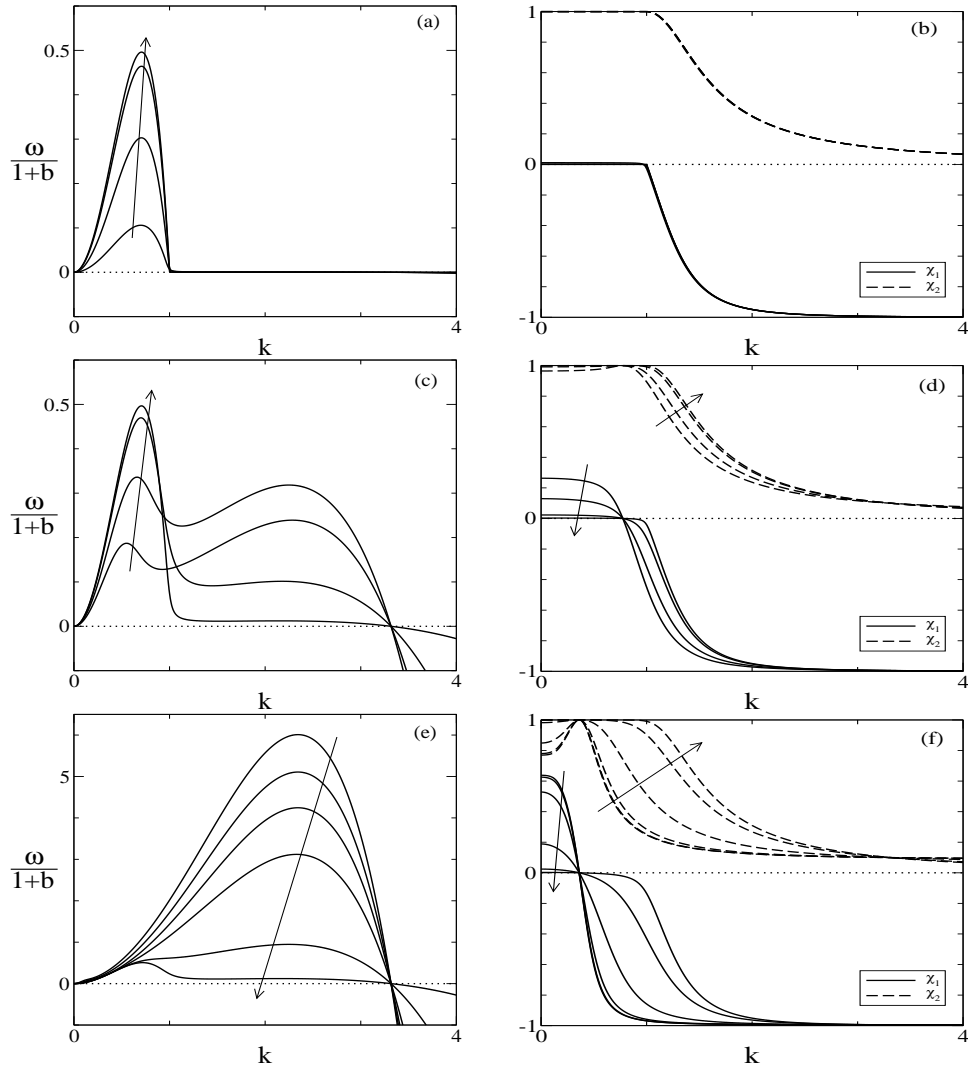


Figure 3: Dispersion relations (left column ((a), (c), (e))) and components of the perturbation vector (right column ((b), (d), (f))) for no slip at the solid-liquid and weak slip at the liquid-liquid interface. Each panel shows graphs for different slip length $b = 0, 1, 10, 100$. The bottom row has two additional values, $b = 1000$ and 10^4 . All arrows point in the direction of increasing b . From top to bottom, the thickness changes from $h_1 = 0.1$ (top), to $h_1 = 1$ (middle) and $h_1 = 10$ (bottom row). Values for other parameters are stated in the main text. Notice that ω has been rescaled by $1+b$ in the left column. The two components χ_1 and χ_2 of the perturbation vector correspond to perturbations of the liquid-liquid and gas-liquid interface, and have been normalised so that $\chi_1^2 + \chi_2^2 = 1$. increasing b .

4.2 Dispersion relation for the strong-slip strong-slip thin film model

We use the same base state and perturbations for the film h_1 and h as in section 3.2. For the the velocities u_1 and u_2 , the base state is zero and thus the perturbed field is

$$u_1(x, t) = \delta u_1^1 \exp(jkx + \omega t), \quad u_2(x, t) = \delta u_2^1 \exp(jkx + \omega t).$$

After expanding, the perturbations of the velocity fields can be eliminated and one obtains the eigenvalue problem

$$\omega \bar{\chi} = k^2 Q_1 T^{-1} Q_2 E \bar{\chi}, \quad (4.6)$$

where $\bar{\chi} = (\chi_1, \chi_2 - \chi_1)$, and the matrices are

$$Q_1 = \begin{bmatrix} h_1 & 0 \\ 0 & 1 \end{bmatrix}, \quad Q_2 = \begin{bmatrix} \beta_1(\mu+1)\beta h_1 & 0 \\ 0 & (\mu+1)\beta \end{bmatrix}, \quad E = \begin{bmatrix} (\sigma+1)k^2 & k^2 \\ k^2 & k^2 + \phi''(1) \end{bmatrix}, \quad (4.7)$$

and

$$T = \begin{bmatrix} -4\mu\beta_1(\mu+1)\beta h_1 k^2 - \mu\beta_1 - \mu(\mu+1)\beta & \mu\beta_1 \\ \mu & -4(\mu+1)\beta k^2 - \mu \end{bmatrix}. \quad (4.8)$$

Therefore, the dispersion relation is given by

$$\omega_{1,2} = -\frac{k^2}{2} Tr(\bar{Q}E) \pm k^2 \sqrt{\frac{Tr(\bar{Q}E)^2}{4} - Det(\bar{Q}E)}, \quad (4.9)$$

where $\bar{Q} = -Q_1 T^{-1} Q_2$.

For the parameters, we assume $\mu = 1$ and $\sigma = 0.1$ as before, $h_1 = 10$, and vary β and β_1 . As before, the value of $|\phi''(1)|$ can be set to $\phi''(1) = -1$, since by rescaling $k = |\phi''(1)|^{1/2} \tilde{k}$, $\omega = |\phi''(1)|^2 \tilde{\omega}$, $\beta = \tilde{\beta}/|\phi''(1)|$, we can remove $\phi''(1)$ from the dispersion relation.

For $\beta = 0.05$, we have, for very small slip parameters at the solid substrate, a bimodal situation. As β_1 is increased, the larger- k maximum dominates, i.e. the instability that mainly affects the liquid-liquid interface in an asymmetric varicose shape. Notice that for the larger β_1 , a very long wave number local maximum emerges in the dispersion relation that is associated with an increasingly symmetric zig-zag shape of the perturbation.

For $\beta = 0.5$ and $\beta = 5$, the situation is similar, except that for the smallest β_1 shown, the dispersion relation has its global maximum in the lower k range where the perturbation only involves the gas-liquid interface. As β_1 is increased, the larger- k maximum takes over with a perturbation that mainly affects the liquid-liquid interface. For very small k , we again observe the emergence of a local maximum as β_1 is increased.

5 Conclusions and Outlook

In this study we have demonstrated, by contrasting two thin-film models for liquid-liquid systems, one in the weak-slip regime and the other in the strong-slip regime, the strong influence of slip on

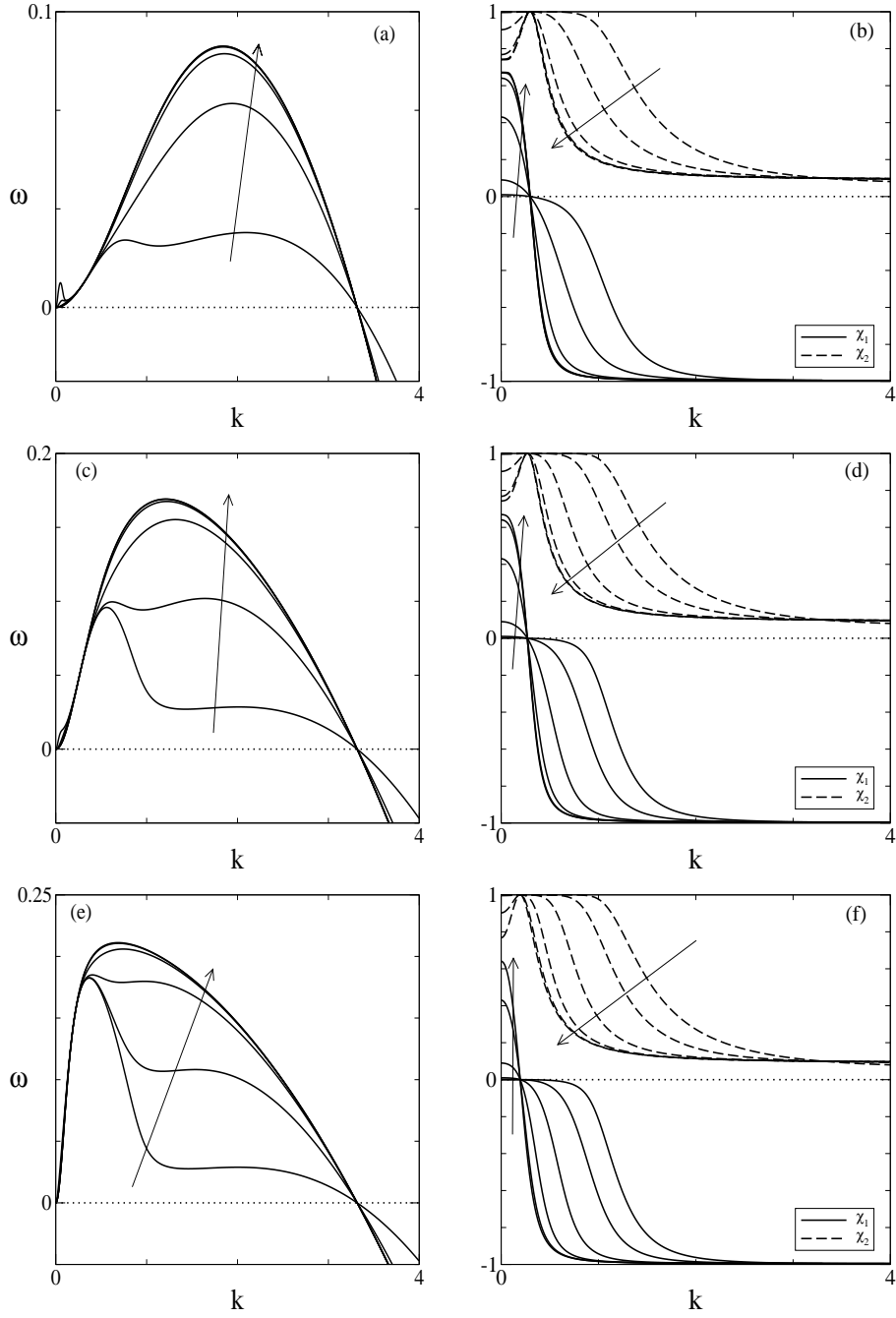


Figure 4: Dispersion relations (left column) and components of the perturbation vector at both interfaces (right column) for $h_1 = 10$ and for $\beta = 0.05, 0.5$, and 5 , from top to bottom. Each subfigure shows the results for different values of $\beta_1 = 10^{-4}, 10^{-3}, 0.01, 0.1, 1, 10$, with the arrows pointing in the direction of increasing β_1 . Values for other parameters are stated in the main text. The two components χ_1 and χ_2 of the perturbation vector correspond to perturbations of the liquid-liquid and gas-liquid interface, and have been normalised so that $\chi_1^2 + \chi_2^2 = 1$.

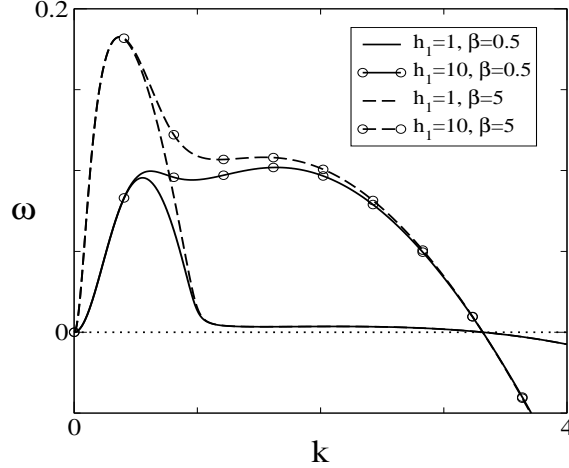


Figure 5: The effect of varying the thickness of the bottom layer for two different values of the slip parameter at the liquid-liquid interface. The other slip parameter is $\beta_1 = 0.001$, and the parameters are as before $\mu = 1$, $\sigma = 0.1$, $h = 1$, and $\phi''(1) = -1$.

the dispersion relations and the dominant shape of the perturbations - i.e how the two interfaces are deformed. It clearly demonstrates that including slip and choosing the appropriate thin film model is vital for comparisons with experimental data and interpreting as well as controlling pattern formation in such systems.

Stability can also be explored directly by linearising and using normal modes for the full model using the Stokes equations. This leads to a more complicated eigenvalue problem for the growth rate that is derived in appendix A, equations (A.7) to (A.16). Numerical solutions of this problem (through a solver for generalised eigenproblems) give the growth rate over the entire parameter space, and by taking corresponding limits the dispersion relations for the thin film models in this paper can be recovered, and further limiting cases can be identified.

In summary, we have demonstrated that increasing slip at the solid substrate generally promotes perturbations of the liquid-liquid relative to the gas-liquid interface, while increasing slip at the liquid-liquid interface favors perturbations at the gas-liquid interface.

If the bottom film layer is thick enough, the preferred wavelength perturbation predominantly affects the liquid-liquid interface, since the maximum of the dispersion relation corresponds to wavenumbers where χ_1 is larger (see figs. 2(e,f)). This interface is softer, i.e. easier to deform than the gas-liquid interface, due to its lower surface tension. The preferred wavelength is determined by the smaller surface tension of this interface. If h_1 is decreased, this instability is suppressed. Instead, another maximum of the dispersion relation at smaller wavenumbers appears and eventually becomes dominant (fig. 2(a)). The case of moderate film thickness h_1 in fig. 2(c) shows both maxima simultaneously. This trend observed for no-slip at the solid-liquid and liquid-liquid interface persists for weak-slip at the liquid-liquid interface, and also for strong slip at both interfaces. Increasing slip at the liquid-liquid interface (and no or fixed slip at the solid substrate) delays the transition in the dispersion relation from one dominant maximum to the other as the thicknesses h_1 is increased. This is also illustrated by fig. 5. For the smaller slip

$\beta = 0.5$, the line with $h_1 = 10$ has two maxima with the one to the right ($k > 1$) being the larger one. In contrast, for $\beta = 5$, a second maximum is just about to form in the graph for $h_1 = 10$, and is clearly dominated by the maximum at $k < 1$.

Changing the slip length at the liquid-liquid interface in the weak-slip regime typically does not have a strong effect on the preferred wave length. In contrast, for strong slip at both interfaces, increasing the slip parameter tends to shift the location of the maxima to lower values, compare figs. 4(a), (c), (e). For one-layer films with strong slip at the liquid-solid interface, a similar tendency and the contrast with weak slip has been observed previously [17, 29].

This paper has focused on the derivation of thin film models for two slip regimes, in order to contrast the different qualitative signatures of the corresponding stability problems. Further interesting combinations of weak-slip, strong-slip as well as intermediate-slip conditions at the interfaces are possible and their impact on patterns and dewetting dynamics will be discussed in future investigations. In addition, the instability discussed here typically gives rise to rupture. In the presence of slip, the self similar solutions have a rich structure even for a one-layer film [30]. We expect that for the two-layer case, this will compound with the additional degrees of freedom arising from the presence of two deformable interfaces.

A Dispersion relations for the Stokes equations

We start the stability analysis with the Stokes equations

$$0 = -\partial_x p_i + \mu_i (\partial_{xx} u_i + \partial_{zz} u_i) \quad (\text{A.1a})$$

$$0 = -\partial_z p_i + \mu_i (\partial_{xx} w_i + \partial_{zz} w_i) \quad (\text{A.1b})$$

$$0 = \partial_x u_i + \partial_z w_i \quad (\text{A.1c})$$

and the boundary conditions from the previous sections. In order to simplify our problem we introduce the stream functions Ψ_1 and Ψ_2 with

$$u_i = \frac{\partial \Psi_i}{\partial z}, \quad w_i = -\frac{\partial \Psi_i}{\partial x} \quad (i = 1, 2). \quad (\text{A.2})$$

Plugging this into the Stokes equations we obtain two biharmonic equations,

$$\partial_x^4 \Psi_i + 2\partial_x^2 \partial_z^2 \Psi_i + \partial_z^4 \Psi_i = 0 \quad (i = 1, 2). \quad (\text{A.3})$$

Linear stability is carried out by introducing small perturbations

$$\left[\Psi_i, h_1 - h_1^0, h_2 - h_2^0, p_i - p_i^0, \phi - \phi_0 \right] = \delta \left[\psi_i(z), \chi, 1, \Pi(z), (1 - \chi) \phi' \Big|_{h^0} \right] \exp(jkx + \omega t) \quad (\text{A.4})$$

around the base state

$$\Psi_i = 0, \quad h_i = h_i^0, \quad h^0 = h_2^0 - h_1^0, \quad p_i = p_i^0, \quad \phi|_{h^0} = \phi_0.$$

where ω and k are the growth coefficient and the wavenumber and obtain

$$\partial_z^4 \psi_i - 2k^2 \partial_z^2 \psi_i + k^4 \psi_i = 0, \quad (\text{A.5})$$

with the general solutions

$$\psi_i(z) = u_{i1} \exp(kz) + u_{i2}z \exp(kz) + u_{i3} \exp(-kz) + u_{i4}z \exp(-kz). \quad (\text{A.6})$$

where the coefficients are determined by using the boundary conditions. First, slip at $z = 0$ leads to

$$(k - b_1k^2)u_{11} + (1 - 2b_1k)u_{12} - (k + b_1k^2)u_{13} + (1 + 2b_1k)u_{14} = 0 \quad (\text{A.7})$$

while impermeability simply reads

$$u_{11} + u_{13} = 0. \quad (\text{A.8})$$

At the free surface $z = h_2$ the kinematic condition becomes

$$ke^{kh_2^0}u_{21} + kh_2^0e^{kh_2^0}u_{22} + ke^{-kh_2^0}u_{23} + kh_2^0e^{-kh_2^0}u_{24} = j\delta\omega \quad (\text{A.9})$$

the tangential stress condition

$$ke^{kh_2^0}u_{21} + (kh_2^0 + 1)e^{kh_2^0}u_{22} + ke^{-kh_2^0}u_{23} + (kh_2^0 - 1)e^{-kh_2^0}u_{24} = 0. \quad (\text{A.10})$$

At the liquid-liquid interface $z = h_1$, the kinematic condition now reads

$$ke^{kh_1^0}u_{11} + kh_1^0e^{kh_1^0}u_{12} + ke^{-kh_1^0}u_{13} + kh_1^0e^{-kh_1^0}u_{14} = j\chi\delta\omega \quad (\text{A.11})$$

the tangential stress condition

$$\begin{aligned} \mu_1[k e^{kh_1^0}u_{11} + (kh_1^0 + 1)e^{kh_1^0}u_{12} + ke^{-kh_1^0}u_{13} + (kh_1^0 - 1)e^{-kh_1^0}u_{14}] \\ - \mu_2[k e^{kh_1^0}u_{21} + (kh_1^0 + 1)e^{kh_1^0}u_{22} + ke^{-kh_1^0}u_{23} + (kh_1^0 - 1)e^{-kh_1^0}u_{24}] = 0. \end{aligned} \quad (\text{A.12})$$

The impermeability condition is equivalent to

$$ke^{kh_1^0}u_{21} + kh_1^0e^{kh_1^0}u_{22} + ke^{-kh_1^0}u_{23} + kh_1^0e^{-kh_1^0}u_{24} = j\chi\delta\omega \quad (\text{A.13})$$

and finally, the slip condition

$$\begin{aligned} ke^{kh_1^0}u_{11} + (kh_1^0 + 1)e^{kh_1^0}u_{12} - ke^{-kh_1^0}u_{13} - (kh_1^0 - 1)e^{-kh_1^0}u_{14} \\ + k(2b_*k - 1)e^{kh_1^0}u_{21} + (kh_1^0 + 1)(2b_*k - 1)e^{kh_1^0}u_{22} \\ + k(2b_*k + 1)e^{-kh_1^0}u_{23} + (kh_1^0 - 1)(2b_*k + 1)e^{-kh_1^0}u_{24} = 0. \end{aligned} \quad (\text{A.14})$$

where $b_* = (1 + \mu_2/\mu_1)b$. For the solution of this algebraic system we put into the remaining boundary conditions, namely the normal stress conditions at $z = h_2$

$$\begin{aligned} j\mu_2[2k^2e^{kh_2^0}u_{21} + 2k^2h_2^0e^{kh_2^0}u_{22} - 2k^2e^{-kh_2^0}u_{23} - 2k^2h_2^0e^{-kh_2^0}u_{24}] \\ = \delta(\sigma_2k^2 + (1 - \chi)\phi''|_{h_2}) \end{aligned} \quad (\text{A.15})$$

and at $z = h_1$

$$\begin{aligned} j\mu_1[2k^2e^{kh_1^0}u_{11} + 2k^2h_1^0e^{kh_1^0}u_{12} - 2k^2e^{-kh_1^0}u_{13} - 2k^2h_1^0e^{-kh_1^0}u_{14}] \\ - j\mu_2[2k^2e^{kh_1^0}u_{21} + 2k^2h_1^0e^{kh_1^0}u_{22} - 2k^2e^{-kh_1^0}u_{23} - 2k^2h_1^0e^{-kh_1^0}u_{24}] \\ = \delta(\sigma_1\chi k^2 - (1 - \chi)\phi''|_{h_1}). \end{aligned} \quad (\text{A.16})$$

B Derivation of the thin film model for strong-slip at the liquid-liquid and solid-liquid interface

We expand the variables in (2.11) as

$$(u_1, w_1, u_2, w_2) = (u_1^{(0)}, w_1^{(0)}, u_2^{(0)}, w_2^{(0)}) + \varepsilon_\ell^2 (u_1^{(1)}, w_1^{(1)}, u_2^{(1)}, w_2^{(1)}) + O(\varepsilon_\ell^4), \quad (\text{B.1a})$$

$$(p_1, p_2) = (p_1^{(0)}, p_2^{(0)}) + \varepsilon_\ell^2 (p_1^{(1)}, p_2^{(1)}) + O(\varepsilon_\ell^4), \quad (\text{B.1b})$$

$$(h_1, h_2) = (h_1^{(0)}, h_2^{(0)}) + \varepsilon_\ell^2 (h_1^{(1)}, h_2^{(1)}) + O(\varepsilon_\ell^4), \quad (\text{B.1c})$$

and consider in turn the leading and next order problem in ε_ℓ .

Leading order problem.

$$0 = \partial_{zz} u_2^{(0)}, \quad (\text{B.2a})$$

$$0 = -\partial_z p_2^{(0)} + \partial_{zz} w_2^{(0)}, \quad (\text{B.2b})$$

$$0 = \partial_x u_2^{(0)} + \partial_z w_2^{(0)}, \quad (\text{B.2c})$$

$$0 = \partial_{zz} u_1^{(0)}, \quad (\text{B.2d})$$

$$0 = -\partial_z p_1^{(0)} + \mu \partial_{zz} w_1^{(0)}, \quad (\text{B.2e})$$

$$0 = \partial_x u_1^{(0)} + \partial_z w_1^{(0)}, \quad (\text{B.2f})$$

For the boundary condition at the free surface $z = h_2^{(0)}$ we get for the normal, tangential and kinematic condition, respectively

$$p_2^{(0)} - \phi'(h^{(0)}) + \partial_{xx} h_2^{(0)} - 2 \left(\partial_z w_2^{(0)} - \partial_z u_2^{(0)} \partial_x h_2^{(0)} \right) = 0, \quad (\text{B.2g})$$

$$\partial_z u_2^{(0)} = 0, \quad (\text{B.2h})$$

$$\partial_t h_2^{(0)} = w_2^{(0)} - u_2^{(0)} \partial_x h_2^{(0)}, \quad (\text{B.2i})$$

For the boundary condition at the free liquid-liquid interface $z = h_1^{(0)}$ we get for the normal, tangential and kinematic condition, respectively

$$p_1^{(0)} - p_2^{(0)} + \phi'(h^{(0)}) + \sigma \partial_{xx} h_1^{(0)} - 2 \left[\left(\mu \partial_z w_1^{(0)} - \partial_z w_2^{(0)} \right) - \left(\mu \partial_z u_1^{(0)} - \partial_z u_2^{(0)} \right) \partial_x h_1^{(0)} \right] = 0, \quad (\text{B.2j})$$

$$\partial_z \left(\mu u_1^{(0)} - u_2^{(0)} \right) = 0, \quad (\text{B.2k})$$

$$\partial_t h_1^{(0)} = w_1^{(0)} - u_1^{(0)} \partial_x h_1^{(0)}. \quad (\text{B.2l})$$

The impermeability condition at $z = h_1^{(0)}$ between the two liquid layers is given by

$$\left(w_2^{(0)} - w_1^{(0)} \right) - \left(u_2^{(0)} - u_1^{(0)} \right) \partial_x h_1^{(0)} = 0 \quad (\text{B.2m})$$

The slip condition at the liquid-liquid interface $z = h_1^{(0)}$ is

$$u_2^{(0)} = \beta \frac{\mu + 1}{\mu} \partial_z u_2^{(0)}. \quad (\text{B.2n})$$

For the boundary conditions at the substrate we assume impermeability and no slip

$$w_1^{(0)} = 0, \quad (\text{B.2o})$$

$$\partial_z u_1^{(0)} = 0. \quad (\text{B.2p})$$

From (B.2d), (B.2p) and (B.2a), (B.2h) we conclude

$$u_1^{(0)} = u_1^{(0)}(x, t), \quad (\text{B.3a})$$

$$u_2^{(0)} = u_2^{(0)}(x, t), \quad (\text{B.3b})$$

thus the horizontal velocity components are independent of z . Using this in (B.2f), (B.2o) and (B.2c), (B.2m) we find

$$w_1^{(0)} = -z \partial_x u_1^{(0)}, \quad (\text{B.4a})$$

$$w_2^{(0)} = -\left(z - h_1^{(0)}\right) \partial_x u_2^{(0)} - \partial_x u_1^{(0)} h_1^{(0)} + (u_2^{(0)} - u_1^{(0)}) \partial_x h_1^{(0)}. \quad (\text{B.4b})$$

Using (B.2e), (B.2j) and (B.2b), (B.2g) we find

$$p_1^{(0)} + 2\mu \partial_x u_1^{(0)} + \partial_{xx} h_2^{(0)} + \sigma \partial_{xx} h_1^{(0)} = 0, \quad (\text{B.5a})$$

$$p_2^{(0)} - \phi' \left(h^{(0)}\right) + 2\partial_x u_2^{(0)} + \partial_{xx} h_2^{(0)} = 0, \quad (\text{B.5b})$$

hence, also independent of z .

Next order problem. To close the problem to leading order and determine an equation for $u_1^{(0)}$ and $u_2^{(0)}$, we need to consider the problem to next order. We will formulate here only the equations that are required to accomplish the task of fixing these leading order velocity components.

The next order upper and lower layer equations in the bulk are

$$0 = -\partial_x p_2^{(0)} + \partial_{xx} u_2^{(0)} + \partial_{zz} u_2^{(1)}, \quad (\text{B.6a})$$

$$0 = -\partial_z p_2^{(1)} + \partial_{xx} w_2^{(0)} + \partial_{zz} w_2^{(1)}, \quad (\text{B.6b})$$

$$0 = \partial_x u_2^{(1)} + \partial_z w_2^{(1)}, \quad (\text{B.6c})$$

$$0 = -\partial_x p_1^{(0)} + \mu \partial_{xx} u_1^{(0)} + \mu \partial_{zz} u_1^{(1)}, \quad (\text{B.6d})$$

$$0 = -\partial_z p_1^{(1)} + \mu \partial_{xx} w_1^{(0)} + \mu \partial_{zz} w_1^{(1)}, \quad (\text{B.6e})$$

$$0 = \partial_x u_1^{(1)} + \partial_z w_1^{(1)}. \quad (\text{B.6f})$$

The next order tangential stress boundary condition at liquid-gas interface $z = h_2^{(0)}$ are

$$\partial_z u_2^{(1)} + \partial_x w_2^{(0)} - 4\partial_x u_2^{(0)} \partial_x h_2^{(0)} = 0, \quad (\text{B.6g})$$

$$\partial_z \left(\mu u_1^{(1)} - u_2^{(1)}\right) + \partial_x \left(\mu w_1^{(0)} - w_2^{(0)}\right) - 4\partial_x \left(\mu u_1^{(0)} - u_2^{(0)}\right) \partial_x h_1^{(0)} = 0. \quad (\text{B.6h})$$

At the liquid-liquid interface $z = h_1^{(0)}$ we have

$$u_2^{(0)} - u_1^{(0)} = \beta \frac{\mu}{\mu + 1} \left[\partial_z u_2^{(1)} + \partial_x w_2^{(0)} - 4 \partial_x u_2^{(0)} \partial_x h_1^{(0)} \right], \quad (\text{B.6i})$$

and at the solid substrate $z = 0$,

$$u_1^{(0)} = \beta_1 \partial_z u_1^{(1)}. \quad (\text{B.6j})$$

In the above equations, we have already made use of the fact that $u_1^{(0)}$ and $u_2^{(0)}$ do not depend on z and dropped all derivatives of these variables with respect to z .

Integrating now (B.6a) and (B.6d), we obtain

$$\partial_z u_2^{(1)} \Big|_{h_2^{(0)}} - \partial_z u_2^{(1)} \Big|_{h_1^{(0)}} = -h^{(0)} \left(-\partial_x p_2^{(0)} + \partial_{xx} u_2^{(0)} \right), \quad (\text{B.7a})$$

$$\partial_z u_1^{(1)} \Big|_{h_2^{(0)}} - \partial_z u_1^{(1)} \Big|_{h_1^{(0)}} = -h_1^{(0)} \left(-\partial_x p_1^{(0)} + \mu \partial_{xx} u_1^{(0)} \right). \quad (\text{B.7b})$$

The pressure terms on the right hand side can be eliminated by using (B.5a) and (B.5b). The terms in the left hand side can be expressed in terms of the leading order solutions $u_2^{(0)}$, $u_2^{(0)}$, $h_1^{(0)}$ and $h_2^{(0)}$ by first using (B.6g), (B.6h), (B.6i) and (B.6j), then eliminating the occurring $w_2^{(0)}$ and $w_1^{(0)}$ via the solutions (B.4a) and (B.4b). This yields the equations (3.8a) and (3.8c). The other two equations, (3.8b) and (3.8d), are obtained by integrating (B.2c) and (B.2f), and using the conditions (B.2i), (B.2l), (B.2m), (B.2p).

References

- [1] F. Brochard Wyart, P. Martin, and C. Redon, Liquid/liquid dewetting. *Langmuir* 9 (1993) 3682–3690.
- [2] A. Pototsky, M. Bestehorn, D. Merkt, and U. Thiele, Alternative pathways of dewetting for a thin liquid two-layer film. *Physical Review E* 70 (2004) 25201.
- [3] A. Pototsky, M. Bestehorn, D. Merkt, and U. Thiele, Morphology changes in the evolution of liquid two-layer films. *The Journal of chemical physics* 122 (2005) 224711.
- [4] L. Fisher and A. Golovin, Nonlinear stability analysis of a two-layer thin liquid film: Dewetting and autophobic behavior. *Journal of colloid and interface science* 291 (2005) 515–528.
- [5] L. Fisher and A. Golovin, Instability of a two-layer thin liquid film with surfactants: Dewetting waves. *Journal of colloid and interface science* 307 (2007) 203–214.
- [6] D. Bandyopadhyay, R. Gulabani, and A. Sharma, Instability and dynamics of thin liquid bilayers. *Ind. Eng. Chem. Res* 44 (2005) 1259–1272.
- [7] D. Bandyopadhyay and A. Sharma, Nonlinear instabilities and pathways of rupture in thin liquid bilayers. *The Journal of chemical physics* 125 (2006) 054711.

- [8] R. V. Craster and O. Matar, On the dynamics of liquid lenses. *J. Colloid and Interface Sci.* 303 (2006) 503–506.
- [9] R. V. Craster and O. Matar, Dynamics and stability of thin liquid films. *Rev. Mod. Phys.* 81 (2009) 1131–1198.
- [10] C. C. Lin, A mathematical model for viscosity in capillary extrusion of two-component polyblends. *Polym. J. (Tokyo)* 11 (1979) 185–192.
- [11] R. Zhao and C. Macosko, Slip at polymer–polymer interfaces: Rheological measurements on coextruded multilayers. *Journal of Rheology* 46 (2002) 145–167.
- [12] H. Zeng, Y. Tian, B. Zhao, M. Tirrell, and J. Israelachvili, Friction at the Liquid/Liquid Interface of Two Immiscible Polymer Films. *Langmuir* (2009) 124–132.
- [13] Z. Lin, T. Kerle, T. Russell, E. Schaffer, and U. Steiner, Electric field induced dewetting at polymer/polymer interfaces. *Macromolecules* 35 (2002) 6255–6262.
- [14] F. Brochard-Wyart and P. de Gennes, Shear-dependent slippage at a polymer/solid interface. *Langmuir* 8 (1992) 3033–3037.
- [15] L. Léger, Friction mechanisms and interfacial slip at fluid-solid interfaces. *J. Phys.: Condensed Matter* 15 (2003) S19–S29.
- [16] E. Lauga, M.P.Brenner, and H. Stone, Microfluidics: The no-slip boundary condition. In: *Handbook of Experimental Fluid Dynamics*. Springer, New York (2007) 1219–1240.
- [17] K. Kargupta, A. Sharma, and R. Khanna, Instability, dynamics and morphology of thin slipping films. *Langmuir* 20 (2004) 244–253.
- [18] A. Münch, B. Wagner, and T. P. Witelski, Lubrication models with small to large slip lengths. *J. Engr. Math.* 53 (2006) 359–383.
- [19] R. Fetzer, K. Jacobs, A. Münch, B. Wagner, and T. P. Witelski., New slip regimes and the shape of dewetting thin liquid films. *Phys. Rev. Lett.* 95 (2005) 127801.
- [20] R. Blossey, A. Münch, M. Rauscher, and B. Wagner, Slip vs viscoelasticity in dewetting thin films. *EPhJ E - Soft Matter* 20 (2006) 267–27.
- [21] T. Vilmin and E. Raphael, Dewetting of thin viscoelastic polymer films on slippery substrates. *Europhysics Letters* 72 (2005) 781.
- [22] R. Fetzer, A. Münch, B. Wagner, M. Rauscher, and K. Jacobs, Quantifying Hydrodynamic Slip: A Comprehensive Analysis of Dewetting Profiles. *Langmuir* 23 (2007) 10559–10566.
- [23] O. Bäumchen, R. Fetzer, and K. Jacobs, Reduced interfacial entanglement density affects the boundary conditions of polymer flow. *PRL* 103 (2009) 247801.
- [24] J. Goveas and G. Fredrickson, Apparent slip at a polymer-polymer interface. *The European Physical Journal B-Condensed Matter and Complex Systems* 2 (1998) 79–92.

- [25] N. P. Adhikari and J. L. Goveas, Effects of slip on the viscosity of polymer melts. *J. Polymer Sci.: Part B: Polymer Physics* 42 (2004) 1888–1904.
- [26] F. Brochard-Wyart and P. de Gennes, Sliding molecules at a polymer/polymer interface. *C. R. Acad. Sci. Ser. II* 327 (1993) 13–17.
- [27] A. Ajdari, Slippage at a polymer/polymer interface: Entanglements and associated friction. *C.R. Acad. Sci., Ser. II* 317 (1993) 1159–1163.
- [28] A. Ajdari, F. B. Wyart, P. G. de Gennes, L. Leibler, J. Viovy, and M. Rubinstein, Slippage of an entangled polymer melt on a grafted surface. *Physica A* 204 (1994) 17–39.
- [29] M. Rauscher, R. Blossey, A. Münch, and B. Wagner, Spinodal dewetting of thin films with large interfacial slip: Implications from the dispersion relation. *Langmuir* 24 (2008) 12290–12294.
- [30] D. Peschka, A. Münch, and B. Niethammer, Thin-film rupture for large slip. *Journal of Engineering Mathematics* 66 (2010) 33–51.